Plasmonics (2013) 8:349–355
DOI 10.1007/s11468-012-9396-7

Infrared Plasmonic Transmission Resonances of Gold Film with Hexagonally Ordered Hole Arrays on ZnSe Substrate

Katherine Cilwa · Shannon Teeters-Kennedy · Keith A. Ramsey · James V. Coe

Received: 14 November 2011 / Accepted: 28 May 2012 / Published online: 8 June 2012

Abstract The high fractional open area of metal thin film coatings, with two dimensional, hexagonally ordered, close packed arrays of holes, makes them of interest for the incorporation of plasmonic effects into a variety of optical devices. Gold films with hexagonal patterns of circular holes have been created on ZnSe infrared windows. The films have 2.50 μm diameter holes and a hexagonal lattice parameter of 3.06 μm which places the primary transmission resonances of the ZnSe/gold interface at ~1,400 cm^{-1} (7.14 μm) and that of the air/gold interface at ~3,800 cm^{-1} (2.63 μm). This geometry produces useful transmission across the whole traditional mid-infrared range. The dispersion of these resonances has been measured by changing the angle of incident light. The data is modeled with explicit momentum matching equations in two different, high symmetry geometries, allowing the effective index of refraction to vary with wavelength. The response of these resonances to the addition of an acetaldehyde coating is described.

Keywords Resonant metal films · Metal films with hexagonal hole arrays on infrared windows · Surface plasmon polaritons in the infrared · Dispersion of transmission resonances · Resonant inductive micromesh

K. Cilwa · S. Teeters-Kennedy · J. V. Coe (✉)
Department of Chemistry, The Ohio State University,
100 West 18th Avenue,
Columbus, OH 43210-1173, USA
e-mail: coe.1@osu.edu

K. A. Ramsey
3007 Rockford Drive,
Columbus, OH 43221, USA

Introduction

Freestanding metal grids (meshes) with arrays of subwavelength holes are useful for plasmonic sensing and enhanced spectra of both coatings and individual subwavelength particles in the holes of the mesh [1–8]. However, patterned metal coatings on window substrates are easier to produce, more stable, and better suited to integration in devices. Thio et al. [9] reported on transmission spectra of hexagonally ordered chromium hole arrays on quartz substrate (0.5 μm holes with 1.0–1.6 μm lattice parameter) in the near infrared (IR) region. They observed primary resonances for both the quartz/metal and air/metal interfaces and gave a smooth metal equation for predicting the resonance positions at perpendicular incidence. Si-Chen Lee et al. [10] reported on hexagonally ordered aluminum hole arrays on silicon substrate (0.5–2.0 μm holes with 3–6 μm lattice parameter). They made dispersion measurements of the transmission resonances, observed interesting splittings when the hole diameters were about half of the lattice parameter, and provided a smooth metal equation for the position of resonances at perpendicular incidence. They observed dispersion of the primary resonance of the Al/silicon interface into either three or four branches. This work makes more detailed dispersion measurements in well specified geometries, provides momentum matching equations which model the dispersion, and enables a more quantitative means of describing the various interactions or splittings observed with surface plasmon polariton (SPP)-mediated transmission resonances.

For more than 30 years, Battelle Memorial Institute has been fabricating metallic mesh thin film coatings on IR windows and domes primarily for electromagnetic shielding against microwave and radiofrequency interference [11]. Such coatings maintain good transmission in the visible

and IR regions. In addition to providing shielding, the metal mesh coatings can be used to resistively heat the surface for defogging or anti-icing [12–14]. Ramsey et al. [11] noted that a mesh coating has resonant transmission when the spacing between the holes is comparable to the incident wavelength. The resonant properties of such meshes were first investigated in the year 1967 by Ulrich [15] in the far infrared; however, the subject caught the scientific community's attention in the year 1998 when the resonances were observed in the visible region by Ebbesen and coworkers [16–18]. Meshes with wavelength-scale lattice parameters can have "superior" IR transmission while still providing good shielding at longer wavelengths [11].

Plasmonic windows have been constructed in this work for utility in IR sensing or spectroscopy. Battelle produced hexagonally ordered gold films with circular holes on several ZnSe windows (3.06 μm lattice parameter, 800 nm Au thickness, 2.50 μm diameter holes). These patterned metal coatings exhibit plasmonic transmission resonances from both interfaces in the traditional range of Fourier transform infrared spectroscopy (FTIR) spectrometers. The gold films with hexagonally ordered hole arrays on ZnSe were investigated at the Ohio State University regarding their plasmonic resonance dispersion properties and response to a thin film dielectric coating. Experimental measurements of the position of transmission resonances vs. angle of incident light (θ) were obtained and modeled with explicit momentum matching dispersion equations in two geometries of high symmetry (angle of incidence changed along the ΓM and ΓK directions of the reciprocal lattice). This work provides a framework for quantifying the strength of various interactions and provides a more detailed guide to the design of potential applications. Unlike freestanding mesh, the metal-coated windows are asymmetric and SPP-mediated resonances can be supported at either the ZnSe/metal interface (not accessible to further coating) or the air/metal interface (which is accessible to further coating). Additionally, the thickness of the gold coating (~800 nm) is small compared to the probing IR wavelengths while the open area (52 %) is a high fraction of the surface area, so the two interfaces may strongly couple both through the holes and through the metal. Resonances from both interfaces were observed, their dispersion was measured and modeled, and their response to a dielectric coating of acetaldehyde is reported.

Production of Hexagonal Metal Films on IR Windows

Gold metal films with hexagonal patterns of circular holes on both 1″ and 2″ diameter ZnSe windows were produced by Battelle's Microfabrication Group. Battelle uses a novel photolithographic process to pattern the micron-sized apertures in the vacuum-deposited gold thin film coating. Figure 1 gives a backlit optical microscope image (left side) and specific geometric details in cross section (right side). The Au coating was 800 nm thick with a 20 nm coating of Cr to better bind the gold to the ZnSe. A 20 nm Ti coating on top helps to protect the Au layer. The NIH software program ImageJ was used to analyze the optical microscope image (Fig. 1, left). Color thresholds and contrast were adjusted until the image was black and white, then the "analyze particles…" function was used to define hole outlines. The program reported on the areas (in pixels^2) of 1,781 holes producing very good statistics. By using a 30 μm scale to convert pixels to μm, the average hole diameter was found to be 2.50±0.01 μm and the average lattice parameter was found to be 3.06±0.01 μm, as limited by the accuracy of the micron to pixel conversion. This mesh consists of 52.4 % open area and the metal coating thickness is only 0.82 μm, so there is great opportunity for coupling of SPPs between interfaces in this asymmetric system (in contrast to freestanding mesh).

Collecting Spectra by Angling the Mesh

The dispersion of the transmission resonances is measured by recording FTIR transmission spectra as a function of the angle (θ) of the mesh relative to spectrometer's beam. The geometry of the first experiment is illustrated in Fig. 2. An optical microscope image is given on the left side of Fig. 2 on which overlays the unit cell's lattice vectors $\left(\vec{a}_1, \vec{a}_2\right)$ in normal space. The coordinates of these vectors are given at

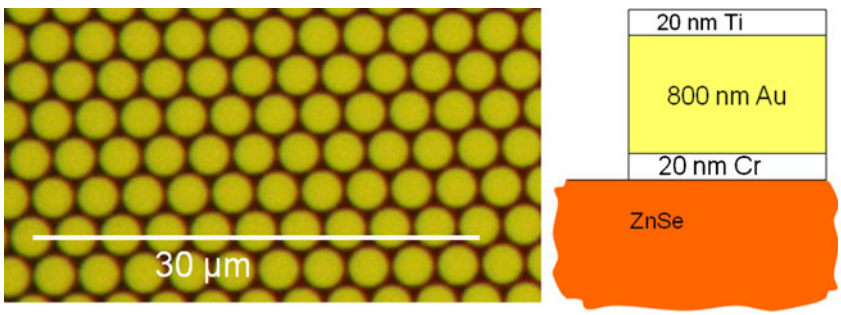

Fig. 1 Backlit optical microscope image of the gold coating with hexagonally ordered holes on ZnSe (*left*). Schematic cross-section showing the thickness of the metallic layers (*right*, not to scale)

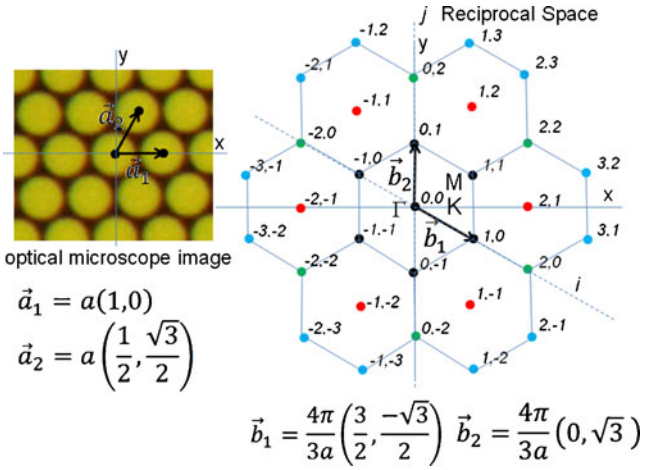

Fig. 2 Optical microscope image (*left*) of Au coating with hexagonally ordered array of holes on ZnSe showing the lattice unit vectors and their coordinates in real space. Schematic drawing of the corresponding diffraction pattern (*right*) showing the lattice vectors in reciprocal space. The ΓK and ΓM directions are indicated on the reciprocal space schematic. In this experiment, the mesh is rotated about the *y*-axis by the angle θ which varies the wave vector of incident light about the *x*-axis in the ΓK direction. At perpendicular incidence, the primary transmission resonance occurs when six diffraction spots (1, 1; 0, 1; −1, 0; −1, −1; 0, −1; 1, 0) are deflected parallel to the metal surface. By changing θ, the primary resonance breaks into three branches which correspond to the vertically aligned spots in the schematic: (1, 0; 1, 1), (0, −1; 0, 1), and (−1, −1; −1, 0)

the bottom left in terms of the *x*- and *y*-Cartesian axes, where *a* is the lattice parameter (a=3.06 μm). A schematic of the diffraction spots in reciprocal space is given on the right side of Fig. 2 along with the reciprocal space lattice vectors $\left(\vec{b}_1, \vec{b}_2\right)$. Notice that a hexagon between the spot centers points up in reciprocal space, i.e., it is rotated by 30° relative to space. A laser pointer was shined through the mesh substrate to verify this orientation. In this experiment, the beam is incident upon the *z*-axis and the mesh is rotated about the *y*-axis by an angle of θ in order to observe dispersion. This means that the component of the incident light along the *x*-axis is changed in the ΓK direction and the wave vector parallel to the surface is $k_x = 2\pi\tilde{\nu}\sin\theta$. Notice that the diffraction spots have been labeled with respect to *i*- and *j*-axes and that the *i*-axis is different than the *x*-axis. Values of *i*, *j* are used to identify the plasmonic transmission resonances that result at wavelengths when diffraction spots are no longer transmitted, i.e., when diffraction spots are bent by 90°, they are no longer transmitted and become evanescent waves at the metal surface. FTIR zero-order transmission spectra were recorded in this geometry in steps of 1° from θ=−5° to 67° with the polarization vertical (0°) and from θ=−5° to 71° with horizontal (90°) polarization as presented in Fig. 3 (showing only spectra with 5° steps). Each spectrum was recorded using a Bruker Equinox 55 FTIR instrument with 100 scans, 4 cm^{-1} resolution, a deuterated triglycine sulfate detector, in ~3 min each.

Next, the sample was rotated by 30° and the experiment was repeated. The diffraction pattern produced by a laser pointer gave hexagons pointing horizontally. A schematic of this orientation is given in Fig. 4 (space on the left, reciprocal space on the right). The component of the incident light along the surface is varied about the *x*-axis in the ΓM direction in this geometry. Again, the wavevector parallel to the surface is $k_x = 2\pi\tilde{\nu}\sin\theta$, but the size of the Brillouin zone is different.

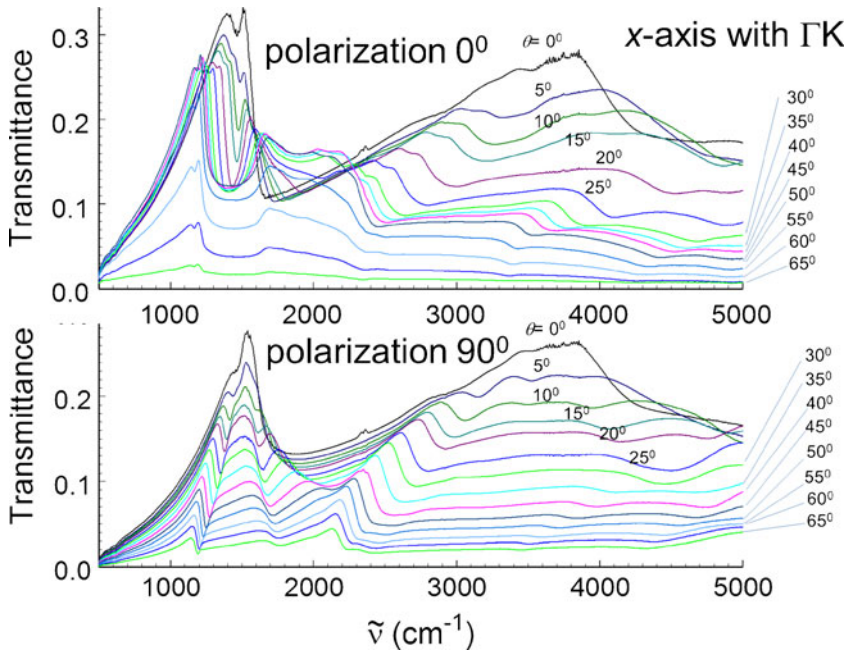

Fig. 3 Transmission spectra vs θ for the geometric arrangement described in Fig. 2, i.e., by varying k_x in the ΓK direction for two polarizations (relative to vertical of Fig. 2). The resonance at perpendicular incidence (θ=0°) in both sets at ~1,400 cm^{-1} is due to the ZnSe/metal interface. The resonance at perpendicular incidence (θ=0°) in both sets at ~3,800 cm^{-1} is due to the air/metal interface

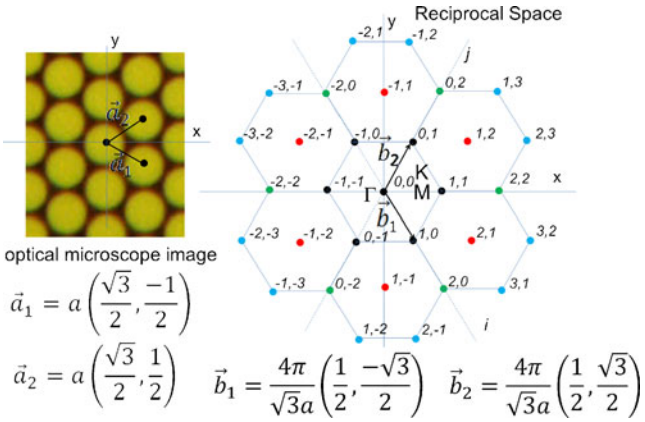

Fig. 4 Rotation of the geometry in Fig. 2 by 30° about the *z*-axis yielded the optical microscope image (*left*) of Au coating with hexagonally ordered array of holes on ZnSe showing the lattice unit vectors and their coordinates in real space. A schematic drawing of the corresponding diffraction pattern (*right*) shows the lattice vectors in reciprocal space. The mesh is rotated about the *y*-axis by the angle θ which varies the wave vector of incident light about the *x*-axis in the ΓM direction. By changing θ, the primary resonance breaks into four branches which correspond to the vertically aligned spots in the schematic: (1, 1), (0, 1; 1, 0), (−1, 0; 0, −1), and (−1, −1)

Diffraction spots (and resonances) were labeled by *i*, *j*, but in this orientation, neither the *i*- or *j*-axes line up with the *x*- and *y*-axes. FTIR zero-order transmission spectra were recorded in this geometry in steps of 1° from θ=0° to 74° for vertical (0°) and horizontal (90°) polarizations as shown in Fig. 5 (only 5° steps). Figures 3 and 5 show that the transmission resonances are clearly sensitive to orientation and polarization. At perpendicular incidence (k_x=0, θ=0°), there are two prominent features: the one at lower wave numbers (~1,400 cm^{-1}) is the primary resonance of the ZnSe/metal interface, while the one at higher wave numbers (~3,800 cm^{-1}) is the primary resonance of the air/metal interface.

Dispersion Diagrams Along the ΓK and ΓM Directions

The spectra were analyzed by finding the positions of transmission resonance maxima at various values of θ. Each spectrum was smoothed and the "peak find" function of the Perkin Elmer Spectrum IR software package was used to find maxima by interpolation (spectra have to be converted to absorption spectra to do this). The peak maximum position and value of θ were used to calculate k_x and the results are plotted in Fig. 6 (*x*-axis aligned with the ΓK direction) and 7 (*x*-axis aligned with ΓM direction).

The half-way point of the first Brillouin zone is indicated with a vertical black line: at $4\pi/(3a)$= 13,689 cm^{-1} with the *x*-axis aligned along the ΓK direction and at $4\pi/(\sqrt{3}a)$= 11,855 cm^{-1} with the *x*-axis aligned along the ΓM direction. At k_x=0 in both plots, the most prominent resonance occurs at ~1,400 cm^{-1} and shows a splitting of ~100 cm^{-1}. This resonance is due to the ZnSe/metal interface. It splits into three main branches with increasing θ when the *x*-axis is aligned with ΓK and it splits into four main branches when the *x*-axis is aligned with ΓM. Both dispersion plots also show a broader peak occurring at ~3,800 cm^{-1} and k_x=0 which is primarily due to the air/metal interface. However, there are also many higher order resonances of the ZnSe/metal interface that overlap with the primary air/metal resonance. So this experiment presents a rich array of opportunities for studying SPP interactions, particularly

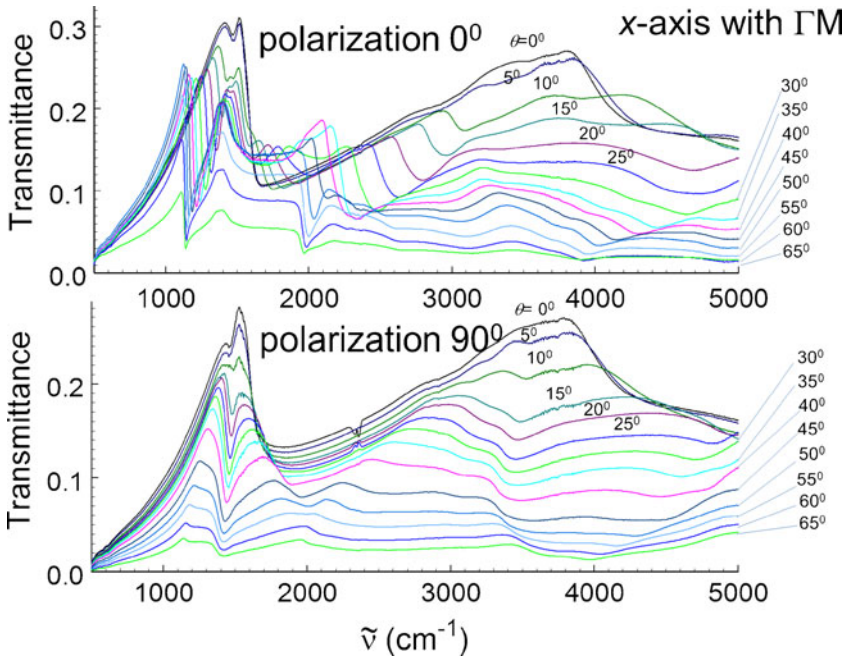

Fig. 5 Transmission spectra vs θ for the geometric arrangement described in Fig. 4, i.e., by varying k_x in the ΓM direction for two polarizations (relative to vertical of Fig. 4). The resonance at perpendicular incidence (θ=0°) in both sets at ~1,400 cm^{-1} is due to the ZnSe/metal interface. The resonance at perpendicular incidence (θ=0°) in both sets at ~3,800 cm^{-1} is due to the air/metal interface

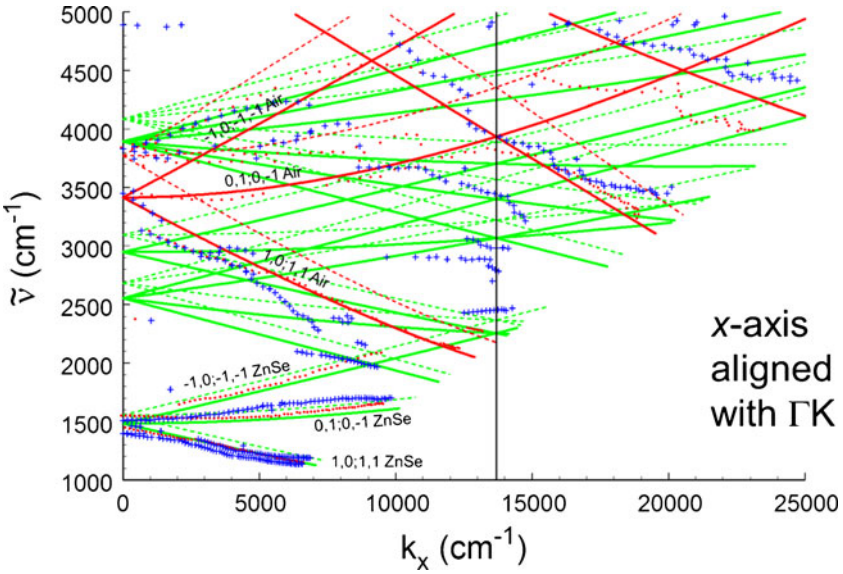

Fig. 6 Dispersion diagram of resonance positions vs $k_x = 2\pi\tilde{\nu}\sin\theta$ for the geometry of Fig. 2 and data in Fig. 3, i.e., with the *x*-axis aligned with the ΓK direction. Note how the primary resonance of the ZnSe/metal interface at k_x=0 and ~1,400 cm^{-1} breaks into three branches. The halfway point of the first Brillouin zone is indicated with a *black vertical line*. The 0° polarization data is denoted with *blue crosses* and the 90° polarization data is indicated with *red circles*

those between the air/metal and ZnSe/metal interfaces. Very interesting polarization behavior and splittings are evident which are better interpreted by virtue of momentum matching dispersion curves.

Momentum Matching Equations for Hexagonal Mesh

Expectation about the position of a resonance is developed with momentum matching equations. Deviations of resonance positions from these predictions help to identify places where the interactions between resonances are strong, such as at band gaps. When light runs along the surface of a metal interacting with the conducting electrons, the mixed state (SPP) gains fermionic character and such mixed states have interactions that are reminiscent of molecules rather than photons or light. Momentum matching equations equate the momentum that incident light would have if the metal film was an homogeneous effective medium with the magnitude of components of incident light and grating steps parallel to the metal surface. Usually, it helps to let the effective index of refraction vary with wavelength which in terms of wave numbers is

$$n_{\text{eff}} = \alpha_0 + \alpha_1\tilde{\nu}^{-1}, \tag{1}$$

where α_0 and α_1 parameterize the wavelength dependence. This allows the momentum matching equations to be solved for $\tilde{\nu}$ as a quadratic. The resonance position when the *x*-axis is aligned with the ΓK direction of the reciprocal lattice is

$$\tilde{\nu}(i,j,\theta)_{\Gamma\text{K}} = \frac{\frac{2i\sin\theta}{\text{a}} - 2\alpha_0\alpha_1 + \sqrt{\left(\frac{2i\sin\theta}{\text{a}} - 2\alpha_0\alpha_1\right)^2 - 4\left(\alpha_0^2 - \sin^2\theta\right)\left(\alpha_1^2\frac{i^2+(2j-i)^2/3}{\text{a}^2}\right)}}{2\left(\alpha_0^2 - \sin^2\theta\right)} \tag{2}$$

Once $\tilde{\nu}$ is determined for a given value of θ, then k_x is determined as $2\pi\tilde{\nu}\sin\theta$. Likewise, the resonance position when the *x*-axis is aligned with the ΓM direction of the reciprocal lattice is

$$\tilde{\nu}(i,j,\theta)_{\Gamma\text{M}} = \frac{\frac{2(i+j)\sin\theta}{\sqrt{3}\text{a}} - 2\alpha_0\alpha_1 + \sqrt{\left(\frac{2(i+j)\sin\theta}{\sqrt{3}\text{a}} - 2\alpha_0\alpha_1\right)^2 - 4\left(\alpha_0^2 - \sin^2\theta\right)\left(\alpha_1^2\frac{\left(\frac{4}{3}\right)(i^2-ij+j^2)}{\text{a}^2}\right)}}{2\left(\alpha_0^2 - \sin^2\theta\right)}. \tag{3}$$

All of the guiding curves shown in Figs. 6 and 7 arise from Eqs. (2) and (3). The light lines at the ZnSe/metal and air/metal interfaces are presented with dotted lines, green for the ZnSe interface and red for the air metal interface. Basically, the 2D periodic hexagonal lattice folds the light lines into space. The fact that the observed resonances follow

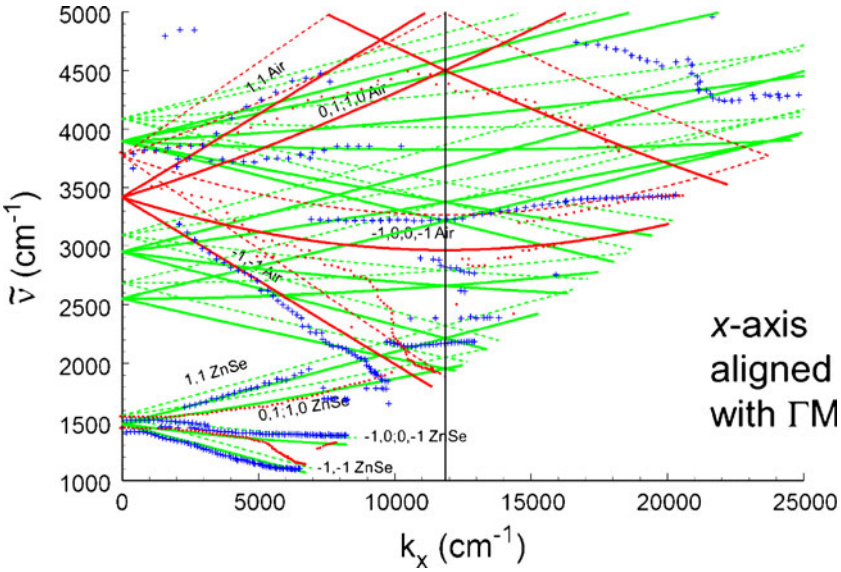

Fig. 7 Dispersion diagram of resonance positions vs $k_x = 2\pi\tilde{\nu}\sin\theta$ for the geometry of Fig. 4 and data in Fig. 5, i.e., with the *x*-axis aligned with the ΓM direction. Note how the primary resonance of the ZnSe/metal interface at k_x=0 and ~1,400 cm^{-1} breaks into four branches. The halfway point of the first Brillouin zone is indicated with a *black vertical line*. The 0° polarization data is denoted with *blue crosses* and the 90° polarization data is indicated with *red circles*

these lines shows their light-like character, while the extent that the observed points push off of these lines reveals their plasmonic character. Using smooth metal considerations, the value of n_{eff} at the ZnSe/metal interface is essentially that of ZnSe (because the magnitude of gold's dielectric permittivity is so much larger than that of the ZnSe). So the parameters are taken as α_0=2.452 and α_1=−43.951 at the ZnSe/metal interface giving n_{eff}=2.420 at 1,350 cm^{-1} and n_{eff}=2.436 at 2,940 cm^{-1} (valid on a limited range from ~1,000–4,500 cm^{-1}). The air/metal interface lines were created with α_0=1.000 and α_1=0 giving a value of n_{eff}=1. Many (but not all) of the observed resonances push off of the light lines to higher values of n_{eff}. The solid green lines in Figs. 6 and 7 refer to the ZnSe/metal interface and were obtained with α_0=2.542 and α_1=−46.149 giving n_{eff}=2.542 and 1,400 cm^{-1} and n_{eff}=2.563 and 3,800 cm^{-1} which are about 0.12 higher in index of refraction than the ZnSe/metal light line. These lines are not a best fit to the data, just a simulation that does a reasonable job of modeling. The solid red lines in Figs. 6 and 7 refer to the air/metal interface and are modeled with α_0=1.121 and α_1=−55.575 giving n_{eff}= 1.081 at 1,400 cm^{-1} and n_{eff}=1.106 at 3,800 cm^{-1} which are ~0.09 higher in index of refraction than the air/metal light line.

There are some interesting splittings and polarization effects. In Fig. 6 (*x*-axis aligned with ΓK), the lowest resonance (labeled 1, 0; 1, 1 ZnSe) occurs with both polarizations, but the 0° polarization branch is split. The second

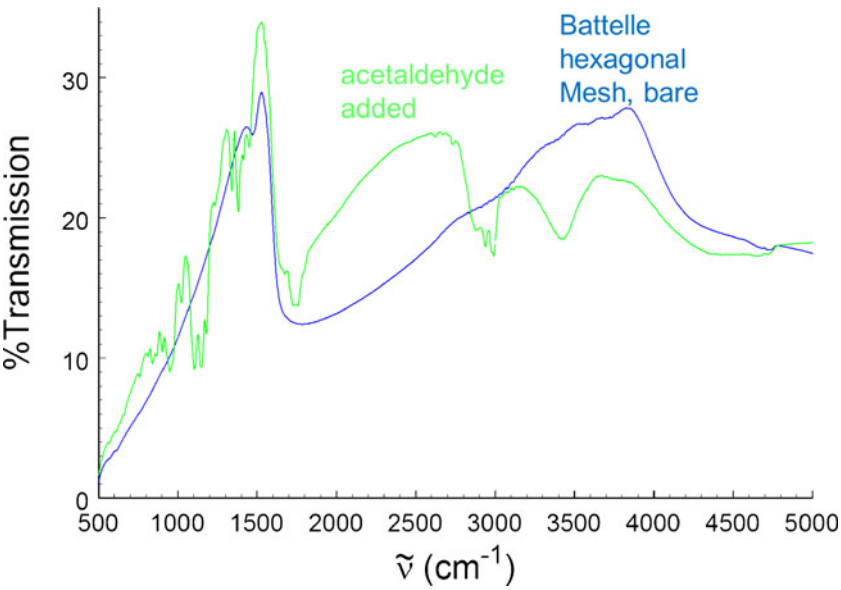

Fig. 8 The zero-order, perpendicular incidence, transmission spectra of gold coated hexagonally ordered hole arrays on ZnSe substrate without (*blue trace* labeled "Batelle hexagonal Mesh, bare") and with a coating of acetaldehyde, CH_3CHO (*green trace* labeled "acetaldehyde added"). The primary resonance of the ZnSe/metal interface at ~1,400 cm^{-1} is not shifted by the coating, but the primary resonance of the air/metal interface at ~3,800 cm^{-1} is shifted to lower wave numbers by ~1,000 cm^{-1}

lowest resonance (labeled 0, 1; 0, −1 ZnSe) occurs with both polarizations, but one is closer to the light line while the other is pulled to a higher value of n_{eff}. The third lowest resonance is only observed with the 90° polarization. In Fig. 7 (x-axis aligned with ΓM), the lowest resonance (labeled −1, −1 ZnSe) and the fourth lowest resonance (labeled 1, 1 ZnSe) occur with just the 0° polarization, while the third lowest resonance (labeled 0, 1; 1, 0 ZnSe) is observed with only 90° polarization. The second lowest resonance (labeled −1, 0; 0, −1 ZnSe) occurs with both polarizations, but as the angle θ is increased, the 90° polarization set jumps off of the trend towards the lowest resonance branch, i.e., at $\tilde{\nu}$ = 1,400 cm^{-1} and k_x=5,000 cm^{-1} (θ=35°), only the 0° polarized is transmitted while both beams were passed at lower θ.

The Effect of a Dielectric Coating

Given that the primary resonance of both the ZnSe/metal and air/metal interfaces are observed in these experiments, the behavior of each resonance was observed as a drop of acetaldehyde (n=1.33) was added to the hexagonal gold-patterned substrate. A zero-order IR transmission spectrum at perpendicular incidence was recorded before the addition and immediately after the addition of acetaldehyde (see Fig. 8). The resonance of the ZnSe/metal interface at ~1,500 cm^{-1} is not shifted, while the resonance of the air/metal interface at ~3,800 cm^{-1} is shifted by about 1,000 cm^{-1} (it is hard to judge exactly because of strong C–H stretching absorption bands). Since the ZnSe/metal interface is not accessible by the addition of a dielectric in the form of solvent, only the resonance of the air/metal interface shifts. It is interesting that the addition of a drop of acetaldehyde solvent increases the transmission of the ZnSe/metal primary resonance even though the peak is not shifted. Films of dielectric can serve to enhance transmission. Finally, note the strong absorptions due to the acetaldehyde molecules. These vibrations can serve as interesting probes with regard to interactions with the SPPs.

Conclusion

It is important to understand the dramatic influence of the ZnSe substrate on the plasmonic behavior of a hexagonal patterned metal coating. In this work, the dispersion of the resonances has been measured in several geometric orientations with two polarizations. Momentum matching equations have been derived which provide a reasonable model of the dispersion data. These equations can be used to predict the positions of resonances for various geometries. While the asymmetry induced by placing a metal patterned coating on a substrate produces a strong primary resonance for each interface (air/metal and ZnSe/metal), only the resonance of the air/metal interface reacts (shifts) with the addition of a coating of dielectric solvent. The higher-order resonances of the ZnSe interface have a high density in the region of the primary resonance of the air/metal interface. They manifest as many extra shoulders on the primary air/metal resonance. Since patterned metal coatings on window substrates are easier to produce, more stable, and better suited to integration in devices, a good understanding of the behavior of the resonances will be useful to those who might like to integrate IR plasmonics with other applications.

Acknowledgments We thank the National Science Foundation for support of this work under grant numbers CHE 0848486 and CHE-0639163.

References

1. Malone MA, Cilwa KE, McCormack M, Coe JVJ (2011) Phys Chem C 115:12250
2. Cilwa KE, McCormack M, Lew M, Robitaille C, Corwin L, Malone MA, Coe JVJ (2011) Phys Chem C 115:16910
3. Malone MA, Prakash S, Heer JM, Corwin LD, Cilwa KE, Coe JVJ (2010) Chem Phys 133:185101
4. Heer J, Corwin L, Cilwa K, Malone MA, Coe JVJ (2010) Phys Chem C 114:520
5. Cilwa KE, Rodriguez KR, Heer JM, Malone MA, Corwin LD, Coe JVJ (2009) Chem Phys 131:061101
6. Coe JV, Heer JM, Teeters-Kennedy S, Tian H, Rodriguez KR (2008) Annu Rev Phys Chem 59:179
7. Coe JV, Rodriguez KR, Teeters-Kennedy S, Cilwa K, Heer J, Tian H, Williams SMJ (2007) Phys Chem C 111:17459
8. Williams SM, Coe JV (2006) Plasmonics 1:87
9. Thio T, Ghaemi HF, Lezec HJ, Wolff PA, Ebbesen TWJ (1999) Opt Soc Am B Opt Phys 16:1743
10. Chang YT, Chuang TH, Tsai MW, Chen LC, Lee SC (2007) J Appl Phys 101
11. Ramsey K, Halman J, Schmalz J, Ruck G (1992) Non-resonant vs. resonant mesh designs for EMI shielding of IR domes. In 4th DoD EM Windows Symposium
12. Halman JI, Ramsey KA, Thomas M, Griffin A (2009) Proc SPIE, 7302, 73020Y/1
13. Ramsey K, Jones S, Halman J, Ruck G (2000) EMI mesh coatings as resistive heating elements for defogging and deicing IR windows. In 8th DoD EM Windows Symposium
14. Ramsey K, Ridgway R, Laudo J, Ruck G, Gorenflo R (1998) Annu Tech Conf Proc–Soc Vac Coaters, 41st, 155
15. Ulrich R (1967) Infrared Phys 7:37
16. Ebbesen TW, Lezec HJ, Ghaemi HF, Thio T, Wolff PA (1998) Nature (London) 391:667
17. Ghaemi HF, Thio T, Grupp DE, Ebbesen TW, Lezec HJ (1998) Phys Rev B 58:6779
18. Schroter U, Heitmann D (1998) Phys Rev B 58:15419